A Unified Mean Velocity Equation of Debris Flows on the Basis of Physical Mechanics: Inspirations from some Arguments and Data collection

Chao Ma[1], Lv Miao[1], Cui Du[2], Liqun Lyu[1]

[1] School of Soil and Water Conservation, Beijing Forestry University, Beijing 100083, China.

[2] School of Civil Engineering, Henan University of Science and Technology, Luoyang 471023, China

Corresponding author: Chao Ma (); ORCID: 0000-0001-8385-0825;

Key Points:

- A combined research was conducted on Manning coefficient, debris flow classification, and mean velocity on basis of mechanical analysis
- Debris flow classification was proposed from the perspective of physical mechanics including friction- and inertial stress-dominated flows
- A new debris flow mean velocity equation was developed from characterizing diameter parameters, density, flow depth, and channel gradient.

Abstract

The physical mechanics and velocity of debris flow are crucial for debris flow mitigation measures. The two aspects closely relate to the grain composition, density, and flow depth. We present a combined research on Manning coefficient, debris flow classification, and mean velocity using mechanical analysis. Comparison of Manning coefficient reveals that it varies greatly at the same observation site and given event. The reciprocal Manning coefficients for viscous flows in Jiangjia Ravine, China, are the highest among the observation sites at a given flow depth. The stony debris flows in Kamikamihorizawa, Japan, are mainly governed by inertial stress, whereas the viscous debris flows in Jiangjia Ravine and Wudu, China, are mainly governed by friction stress. The reciprocal Manning coefficient of stony debris flows in Kamikamihorizawa, but not of viscous debris flows in China, increases with increasing Savage and Bagnold numbers. The reciprocal Manning coefficient decreases with the Friction number for both viscous and stony debris flows. Based on dimensionless parameters, we proposed debris flow classification from the perspective of physical mechanics including friction- and inertial stress-dominated flows. Finally, a new debris flow mean velocity equation was developed considering the characterizing diameter parameters (D_{50}, D_{10}), density, flow depth, and channel gradient. This equation performs well and could be updated in the future if the observed data of friction- and inertial stress-dominated flows are available. The results of this work can help strengthen the resistance of debris flows in different flow regimes.

Keywords: Physical mechanics; Manning coefficient; Dimensionless parameters; Roughness

1 Introduction

Debris flows are solid and water mixtures surging down slopes in response to gravitational attraction (Iverson, 1997; Takahashi & Das, 2014). They generally have densities comparable to those of rock avalanches and other types of landslides (Johnson, 1970; Yong et al., 2013). Their occurrence has greatly increased in the last few decades due to strong earthquake, fire hazards, glacier retreat, and extreme rainstorms (Breien et al., 2008; Cui et al., 2018; Li et al., 2019; Ma et al., 2017; McCoy et al., 2010; Wang et al., 2021). Resulting from the various particle component, their physical mechanics are very complex, which alters their dynamics properties in time and space (Pierson, 1985).

Mean velocity is one of the most important parameters in designing of mitigation structures. It is commonly back-calculated from super-elevation events or Manning–Strickler equation. Velocity back-calculations are mainly based on forced vortex equation (French, 1985; Hungr et al., 1984; Johnson, 1970). Generally, Manning coefficient represents the total resistance of debris flow and is closely related to the flow depth (Fei, 2003; Kang, 1985). Rickenmann and Zimmermann (1993) have suggested that the mean value of Manning coefficient is about 0.1, while Fei and Shu (2004) have suggested a mean value of 0.033. The Manning–Strickler approach shows that Manning coefficient is proportional to the 1/6 power of grain diameter (Julien, 2010; Julien & Paris, 2010); the coefficient is 0.067 for water flows and 0.1 for laboratory and field debris flows (Rickenmann, 1999). However, some natural debris flow observation sites reveal that Manning coefficient differs across various flow types (Fei & Shu, 2004; Kang et al., 2004) and regions (Fei & Shu, 2004). Julien and Paris (2010) reveals that the ratio of mean velocity to shear velocity slightly increases as the logarithmic relative roughness. However, the velocity ratio may increase for cohesionless flows (Hashimoto & Hirano, 1997) and decrease for viscous or muddy flows (Yu, 2012). By classifying grain contact friction regime and collision regime, Hashimoto and Hirano (1997) found that the velocity ratio in intergranular stress-dominated flow is smaller than inertial stress-dominated flow. Simultaneously, velocity ratio abruptly increases at smaller relative roughness and slightly increases or decreases thereafter. This implies that the flow resistance is closely related to the dominant stress or the relative importance of grain-to-grain interaction.

The integrated flow resistance of debris flows is derived from viscous shear, grain contact friction, grain collision, and boundary surfaces (Armanini et al., 2009; Coussot & Meunier, 1996; Cui et al., 2016). Therefore, the ratio between mean and shear velocities merely represents the shear resistance, which is part of flow resistance. Takahashi and Das (2014) revealed that debris flows in Kamikamihorizawa, Japan, exhibits smaller shear resistance than those in Jiangjia Ravine, China, and Nojiri and Mizunashi Rivers, Japan, where the debris flows are of viscous or turbulent-muddy type. The stony flows in Kamikamihorizawa are characterized as relatively coarse sediment and muddy water such that the internal stresses generated by grain collision support their movement. For the other three flows, viscous or friction stress may dominate their movement. Therefore,

the various dominated stresses may control flow resistance. The Manning coefficient or the ratio of mean velocity to shear velocity may indicate the relative importance of the aforementioned multiple stress.

This study aims to understand the Manning coefficient n of debris flows in some natural observation sites worldwide and the flow resistance with respect to the relative importance of stress. Further, the range of n of debris flows and the relationship between mean velocity and flow depth was studied. From the observed debris flows at Jiangjia Ravine and Wudu, China, and Kahikahihorizawa, three dimensionless numbers, representing the ratio of inertial grain collision to grain contact friction and viscous shear and the ratio of grain contact friction to viscous shear, were analyzed to correlate the n and the ratio of mean velocity to shear velocity. The ratio of the velocity ratio to n was also put forward in this work to examine the ratio of shear resistance to integrated resistance. The results of this work can be useful to further the knowledge on the flow resistance of debris flows with varying bulk densities.

2 Materials and Methods

2.1 Mean velocity equation

Generally, the approaches estimating mean velocity of debris flows is derived from Manning–Strickler method (Table 1). Based on long-term observation work in Jiangjia Ravine, Yunnan Province, Southern China, Kang (1985) found that the Manning coefficient strongly relates to the flow depth, and Fei (2003) updated expressions of Manning coefficient. The expression proposed by Fei (2003) illustrates that the resistance of debris flow depends on multiple parameters, which include flow depth, volume fraction, characterizing diameter of 10-percentle size, and channel gradient. Considering debris flow travel at open wide channel, Hu et al. (2013) proposed an approach considering the flow width, flow depth, and channel gradient. Liu et al. (2020) proposed two parameters representing the effect of characterizing diameter and density on debris flow velocity.

Julien and Paris (2010) collected global debris flow velocity data and developed an equation involving the shear velocity, flow depth, and characterizing diameter equal to 50-percentile size. However, this method may fail to explain the reason the velocity ratio increases with relative roughness for cohesionless flow, while decreases for mud flow or viscous flow. Additionally, it does not consider the effect of debris flow density and solid fraction. Yu (2012) further discussed the issue and proposed an equation involving two grain size diameters, which include 50- and 10-percentile particle size. The equation proposed by Yu (2012) can explain the laws that velocity ratio decreases with relative roughness for mud flow or viscous flow. The discussions of Yu (2012) and Julien and Paris (2010), together with the works of Fei (2003) and Liu et al. (2020) imply that the dominate stress of mud/viscous and stony flows are completely different. It is common knowledge that in debris flow contains varying size of particles, the cause of resistance mainly depends on the particle-to particle interaction,

other than flow boundary. Therefore, the magnitude of Manning coefficient may link the relative importance of particle interaction and particle-fluid interaction. Summarily, it seems that two characterizing diameter parameters (D_{50} and D_{10}, in mm), solid fraction (v_s), flow depth (h, in m), and channel gradient (J) should be considered in deriving the mean velocity equation of debris flows.

2.2 Debris flow physical mechanics analysis

Another way to develop the mean velocity of debris flow can be from mechanical analysis. Generally, the dispersive and frictional stresses between solid particles, viscous shear stress, and turbulence of pore fluids play an important role in governing debris flow dynamics. Among the multiple stress types, grain contact friction (particle-particle interaction), inertial grain collision (particle-particle interaction), and viscous shear (fluid-fluid interaction) have a greater impact on the resistance of debris flow. To quantify their relative contributions to the movement of debris flow, dimensionless parameters are introduced, which include Savage (N_{Sav}), Bagnold (N_{Bag}), and Friction numbers (N_{Fric}).

Bagnold number N_{Bag} characterizes the ratio between inertial grain collision and viscous shear stress:

$$N_{\mathrm{Bag}} = \frac{\rho_s \gamma D_{50}^2}{\mu} \times \frac{v_s}{1-v_s} \#(1)$$

Savage number N_{Sav} characterizes the ratio of inertial grain collision stress to grain contact friction stress:

$$N_{\mathrm{Sav}} = \frac{\rho_s \gamma D_{50}^2}{(\rho_s - \rho_f)\mathrm{gh}\tan\varphi} \#(2)$$

The Friction number N_{Fric} represents the ratio of grain contact friction stress to viscous shear stress:

$$N_{\mathrm{Fric}} = \frac{(\rho_s - \rho_f)\mathrm{gH}\tan\varphi}{} \times \frac{v_s}{1-v_s} \#(3)$$

where, ρ_s is the density of solid particles ($\frac{\mathrm{kg}}{m^3}$), $\rho_f$is the density of the fluid phase ($\frac{\mathrm{kg}}{m^3}$), D_{50} is the mean diameter of the solid phase (m), μ is the dynamic viscosity of interstitial fluid ($\mathrm{Pa} \bullet s$), v_s is the solid phase volume fraction, and φ is the internal friction angle (°).

Some of parameters in the formula are calculated as follows:

$$\gamma = \frac{v}{h} \#(4)$$

$$V_2 = \frac{C_v \times P_{(2)}}{100} \#(5)$$

$$v_s = C_v \times (1 - V_2) \#(6)$$

$$V_{\text{fine}} = \frac{C_v \times V_2}{1 - C_v + C_v \times V_2} \#(7)$$

$$\rho_f = \rho_s \times V_{\text{fine}} + 1000 \times (1 - V_{\text{fine}}) \#(8)$$

where, V_2 is the fluid phase involving solid particles of D<2mm, $P_{(2)}$ is the fraction of particles of D<2mm, and V_{fine} is the volume fraction of silt and clay in the fluid phase.

Based on the results of the USGS flume tests, Iverson (1997) proposed the critical values of three dimensionless parameters to characterize the transition interval from one stress to another. For example, when the contribution of inertial grain collision to the movement of debris flow exceeds the viscous shear stress, the value of $N_{\text{Bag}} > 200$, when $N_{\text{Sav}} > 0.1$, the contribution of inertial grain collision exceeds the grain contact friction, and when $N_{\text{Fric}} > 2000$, the contribution of grain contact friction exceeds the viscous shear (Iverson, 1997).

3 Results

3.1 Manning coefficient vs flow depth

Table 2 shows the observed flow depth, mean velocity, and reciprocal Manning coefficient of debris flows in some observation sites. Although the R^2 of some power-law relationships between flow depth and Manning coefficient is low, the data scatter can be used to compare the differences in resistance.

Figure 1 shows the flow depth, velocity, and Manning coefficient of some debris flows in the European Alps and USA. Figure 1a shows that the velocity increases with flow depth, and the debris flows at Chalk cliffs travel faster than other flows at the given flow depth. Du et al. (1987) and Shu and Fei (2003) developed two empirical formulas, displayed as blue and red lines in Figure 1b, from the observed debris flows in Jiangjia Ravine. The two lines are located above other data scatter indicating that the reciprocal Manning coefficient in Jiangjia Ravine is higher at the same flow depth. Figure 2 shows the observed debris flow data at the Ohya landslide and Kamikamihorizawa. The debris flows at the Ohya landslides travel faster than that at Kamikamihorizawa (Figure 2a), and the reciprocal Manning coefficients are not different each other (Figure 2b).

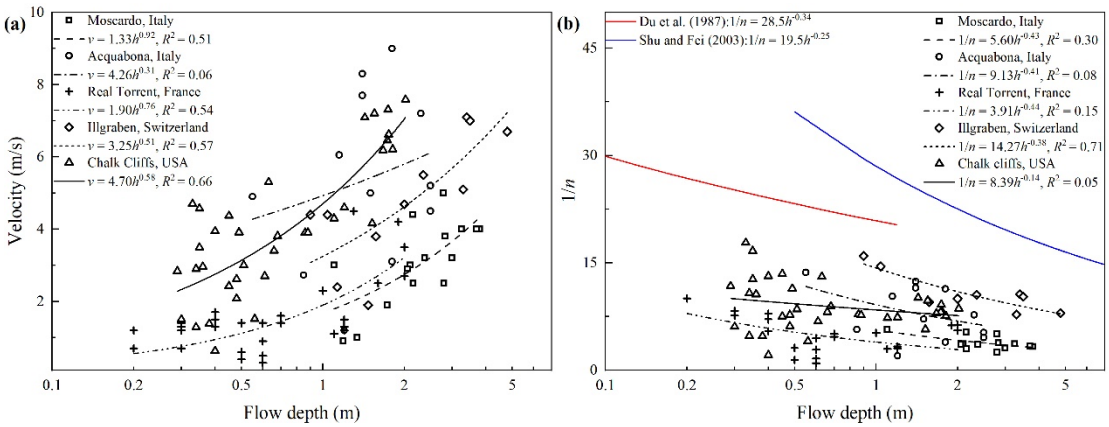

Figure 1. Plots depicting the debris flow velocity and Manning coefficient vs flow depth at some observation sites in Europe and USA.

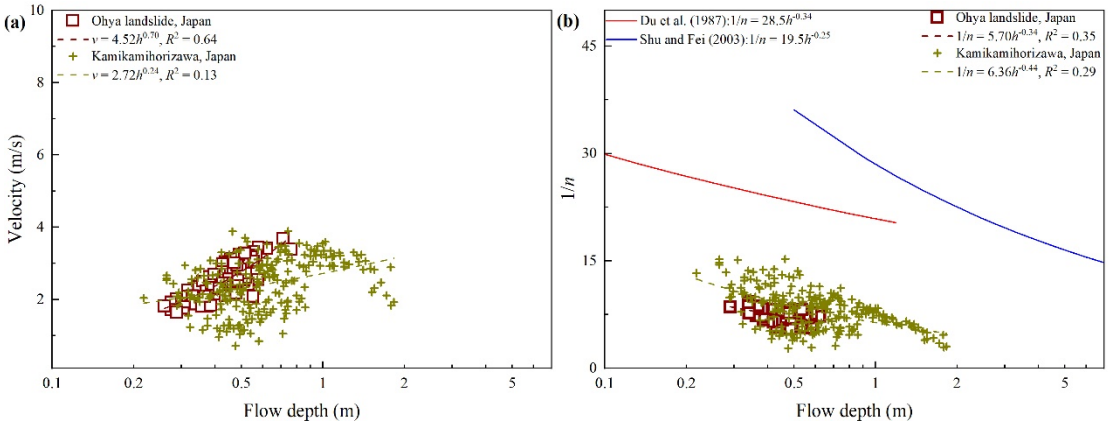

Figure 2. Plots showing the debris flow velocity and Manning coefficient vs flow depth at two observation sites in Japan.

Debris flows in Jiangjia Ravine travel faster than that at Wudu at the given flow depth (Figure 3a), and the reciprocal Manning coefficients for viscous flows in Jiangjia are relatively higher (Figure 3b). According to the observed debris flow data in Table 2, the back-estimated Manning coefficient is highly changeable and can be different at the same observation site and debris flow event. As debris flows contain debris of various sizes, the resistance should strongly be related to a specified dominated stress. Therefore, the relationship between Manning coefficient and aforementioned dimensionless numbers needs to be further examined.

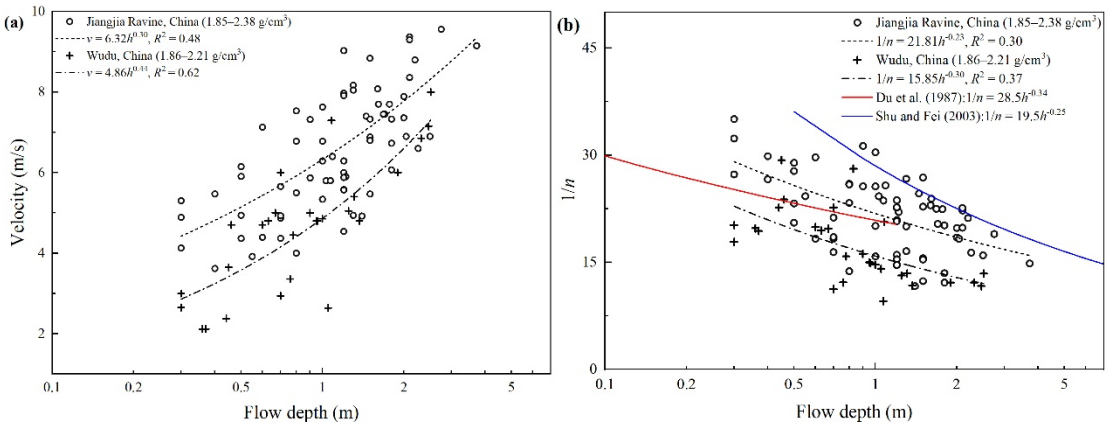

Figure 3. Plots depicting the debris flow velocity and Manning coefficient vs flow depth at two observation sites in China

3.2 Manning coefficient vs dimensionless parameters

3.2.1 Bagnold number

Table 2 merely lists some available velocity and flow depth, while other data, such as the particle component and channel gradient, are not available to calculate the three dimensionless numbers. Therefore, the observed data from Jiangjia Ravine, Wudu, and Kamikamihorizawa are used (Table 3, Takahashi & Das, 2014). Debris flows in Jiangjia Ravine and Wudu have more fine and less coarse grains than the stony debris flows in Kamikamihorizawa (Kang et al., 2004; Takahashi, 2007). This may result in the differences in dominated stress and the values of dimensionless numbers. Bagnold number represents the ratio between grain collision and viscous shear stress. The transitional value is appoximately 200, as suggested by Iverson (1997). The Bagnold number of the viscous debris flows in Jiangjia Ravine and Wudu are much smaller than the critical value, indicating that the viscous shear stress is dominant over inertial grain collision. For the stony debris flows in the Kamikamihorizawa Japan, the values of Bagnold number are higher than the critical value (Figure 4) indicating that the dispersive stress generated by inertial grain collision dominate over viscous shear.

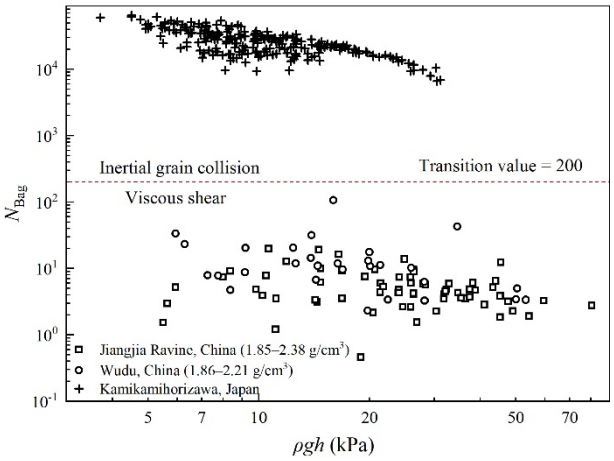

Figure 4. Plot displaying the Bagnold number vs normal stress for debris flows in Kamikamihorizawa Japan, and Jiangjia Ravine and Wudu, China

Furthermore, the relationships between Manning coefficient and Bagnold number for viscous debris flows in China and stony flows in Japan are different (Figure 5). The reciprocal Manning coefficient for stony debris flows in Kamikamihorizawa increases with Bagnold number, indicating that the resistance component from particle collision is more important than viscous shear stress. In fact, the viscous stress mainly comes from the fluid phase, and the stony debris flows in Kamikamihorizawa lack fine grains. Therefore, the Bagnold number can distinguish the viscous debris flows in Jiangjia Ravine and Wudu, and the stony debris flows in Kamikamihorizawa. Additonally, no such positive relationship exists in viscous debris flow indicating that the main resistance component is not from particle collision.

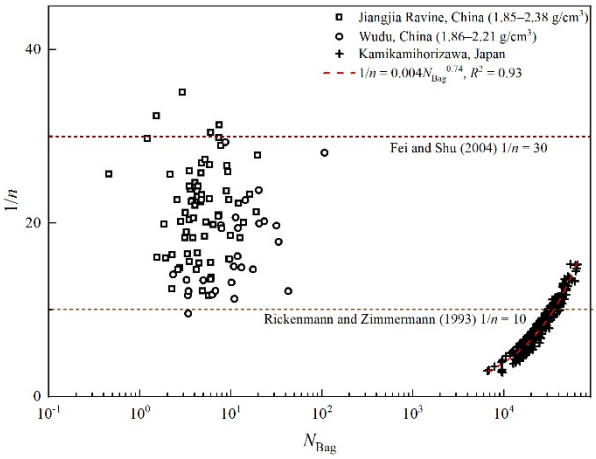

Figure 5. Plot showing the Bagnold number vs Manning coefficient for debris

flows in Kamikamihorizawa, Japan, and Jiangjia Ravine and Wudu, China

3.2.2 Savage number

The values of Savage number of debris flows in Jiangjia Ravine and Wudu are much smaller than the critical value ($N_{Sav} < 0.1$) (Figure 6). Specifically, the contribution of friction stress to the movement of viscous debris flows exceeds the inertial stress. Additionally, the majority of the observed stony debris flows at Kamikamihorizawa are dominated by inertial stress and minor flows are dominated by frictional stress. Both the Bagnold and Savage numbers decrease as the normal stress of debris flows increases, indicating that the contribution of inertial stress decreases as the contribution of frictional and viscous shear stresses increases.

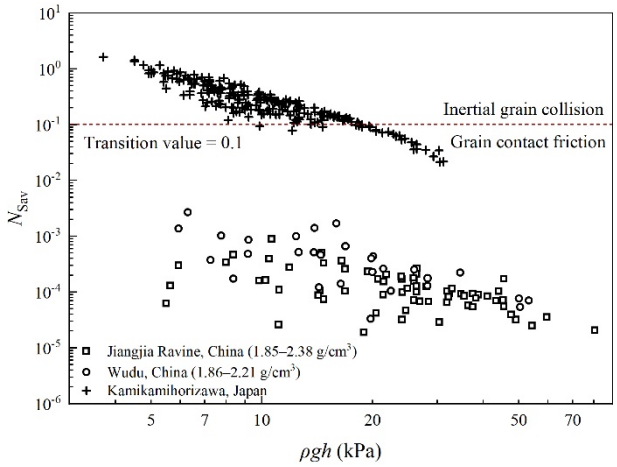

Figure 6. Plot showing the Savage number vs normal stress for debris flows in Kamikamihorizawa, Japan, and Jiangjia Ravine and Wudu, China

Similar to the relationship between Bagnold number and Manning coefficient, the reciprocal Manning coefficient of stony debris flows in Kamikamihorizawa increases with the Savage number; however, this is not observed for viscous debris flows in China (Figure 7). Therefore, the main resistance component for viscous debris flow is not from inertial stress, but friction or viscous shear stresses.

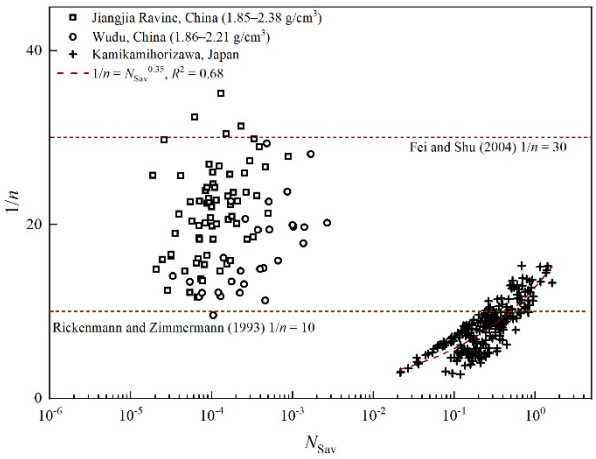

Figure 7. Plot showing the Savage number vs Manning coefficient for debris flows in Kamikamihorizawa, Japan, and Jiangjia Ravine and Wudu, China

3.2.3 Friction number

Friction number represents the relative importance of friction stress to viscous shear for debris flow dynamic properties. In comparison, the friction stress seems to play a dominant role for both stony debris flows in Kamikamihorizawa and viscous debris flow in China (Figure 8). The Friction numbers of debris flows in Kamikamihorizawa increase with total stress, and the majority of flows in Jiangjia Ravine and Wudu are governed by frictional stress. Therefore, the dynamics of stony debris flows in Kamikamihorizawa are mainly governed by inertial stress and partially by friction stress. The viscous debris flows in Jiangjia Ravine and Wudu are mainly governed by frictional stress and partially by viscous shear stress. The contribution of particle collision to debris flow dynamics in the Jiangjia Ravine and Wudu may play a third role as the debris flows in the two areas contain more fine grains and their viscosities are higher than that of the stony debris flows in Kamikamihorizawa.

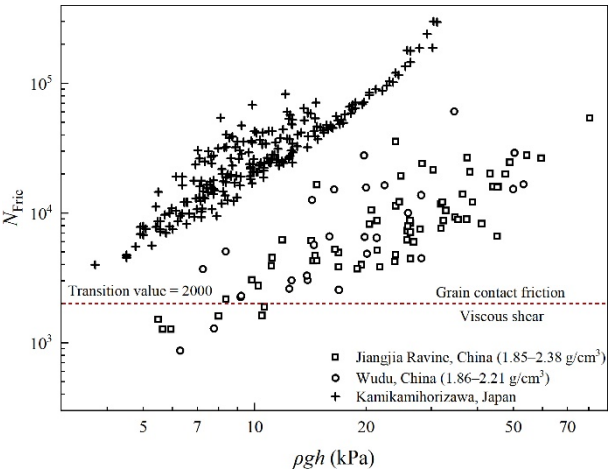

Figure 8. Plot showing the Friction number vs normal stress for debris flows in Kamikamihorizawa, Japan, and Jiangjia Ravine and Wudu, China

The reciprocal Manning coefficient decreases with the Friction number for both viscous and stony debris flows, as shown in Figure 9. At a given friction number, the reciprocal Manning coefficient of viscous debris flows in Jiangjia Ravine is higher than that of viscous flows in Wudu and stony flows Kamikamihorizawa. As the Friction number increases, the values of Manning coefficient increases. This indicates that the main component of resistance within debris flows may be from particle contact friction. Additionally, the reciprocal Manning coefficient of viscous flows ranges from 10 to 30. The reciprocal Manning coefficient of stony flows in Kamikamihorizawa are much less than 10, as suggested by Rickenmann and Zimmermann (1993).

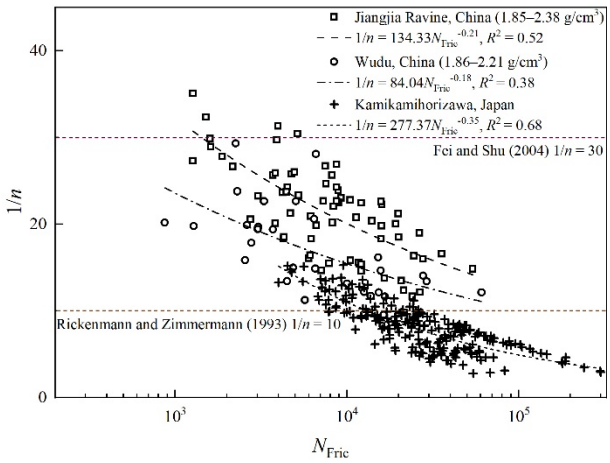

Figure 9. Plot showing the Friction number vs Manning coefficient for debris flows in Kamikamihorizawa, Japan, and Jiangjia Ravine and Wudu, China

3.2.4 Revised Friction number

Figure 9 also indicates that the grain composition of debris flows plays a non-ignorable influence on the resistance. In natural conditions, both the grain composition of debris flows and substrate sediments contribute to the resistance, which include the component of interior flow body, and interaction between flow bottom and substrate grains. Specifically, the Manning coefficient of a debris flow is composed of the external and internal roughness indices (Zhu et al., 2020).

The relative roughness (D_{50}/H) was proposed in developing the mean velocity of debris flows (Julien & Paris, 2010). Actually, the D_{50}/H merely indicates the high ratios of grain diameter to flow depth, or the roughness component from coarse grains for either stony or viscous debris flows. Another physical meaning of relative roughness is that it reflects the relative contact area of large grains to flow column. The shortage of this relative roughness may not reflect the relative contact area of fine grains (e.g., D_{10}/H) to the flow column. For viscous debris flows, the proportion of grains have two main components, while the proportions of grain in stony flows have one component (Kang et al., 2004; Takahashi, 2007). During the interaction between flow bottom and the substrate bed, the relative contact area of fine grains to flow column acts more profoundly than the large grains for viscous flows. In Figure 9, the Manning coefficient of viscous debris flows is minimal in Jiangjia Ravine, followed by Wudu and Kamikamihorizawa. The difference in the decreasing tendency of reciprocal Manning coefficient with Friction number in Figure 9 may be attributed to the effect of fine grains, as the friction number merely represents the ratio between total friction stress to viscous shear stress from fluid phase. Therefore, a new dimensionless number, D10/H×Nfric, is proposed in this study to further examine its relationship with Manning coefficient.

Further regression analysis reveals that the reciprocal Manning coefficient exhibits a decreasing power-law relationship with the revised dimensionless number, and the R^2 is 0.73 (Figure 10). Specifically, the Manning roughness coefficient increases with the new dimensionless number. If the friction stress from the relative contact area of fine grains accounts for higher proportion, the Manning roughness coefficient resistance greatly increases. This coefficient and the exponent in the power-law expression could be further updated because the available particle component and bulk density of stony debris flows in Kamikamihorizawa are few (Takahashi, 2007).

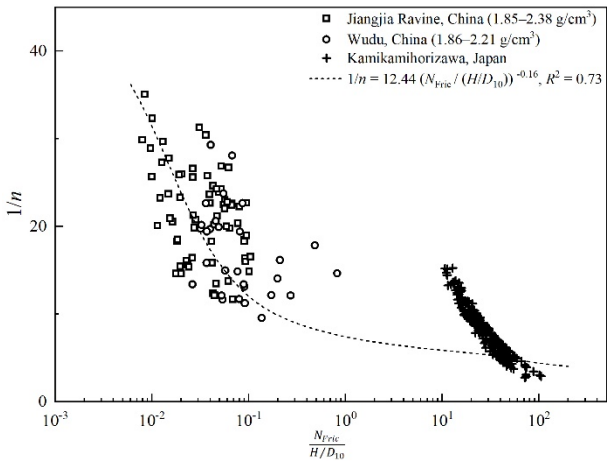

Figure 10. Plot exhibiting the revised friction number vs Manning coefficient for debris flows in Kamikamihorizawa, Japan, and Jiangjia Ravine and Wudu, China

3.2.5 Comparison of dimensionless parameters

The physical meanings of the three dimensionless numbers cannot help examine the dominant stress within debris flows and main resistance component, but it helps in classifying debris flows from the perspective of physical mechanics. Generally, debris flow classification commonly base on the appearance, sediment concentration, coarse and fine sediments, hydraulic features, viscousity, or a combination of them (Coussot & Meunier, 1996; Cui et al., 2016; Du, 2021; Imaizumi et al., 2005; Okano et al., 2012; Takahashi, 2007). It is difficult to identify the main resistance component within debris flows and it is necessary to classify debris flows by the dominated stress.

Table 4 lists the values of the three dimensionless numbers of debris flows globally. According to the values of the three numbers and their transition suggested by Iverson (1997), debris flows in the 13 sites can be briefly divided into two types, which include friction- and inertial stress-dominated flow. Particularly, majority of debris flows are friction stress-dominated flow including Oddstad, South Toutle River, Osceola, Illgraben, Jiangjia Ravine, Houyenshan, and Wudu. The inertial flows contain Acquabona, Moscardo, Chalk Cliff, and Kamikamihorizawa. Physical mechanics-based classification can help understand the main resistance component and be helpful for numerical simulation works using suitable rheology models.

3.3 Mean velocity of debris flow

Based on the proposed definition of inter-granular stress in the shear flows of fluid-solid mixtures and dry granular materials (Bagnold, 1954; Savage & Hutter, 1991), Hashimoto and Hirano (1997) classified the hyperconcentrated sand-water mixture into two sublayers, which include inertial sublayer and granular

layer, and introduced a dimensionless parameter similar to the Savage number:

$$\frac{u}{u_*} = \left(\frac{H}{D_{50}}\right)\sqrt{\frac{\rho_f}{(\rho_s F(C))}} \#(9)$$

where, $F(C) = \left(\frac{C}{C_*}\right)^2/(1-\frac{C}{C_*})$, C the volume fraction of silt and clay in the fluid phase, C_* is the maximum possible concentration, u the mixture velocity, and u_* the shear velocity (e.g., $\sqrt{\mathrm{gHJ}}$).

The physical meaning of this parameter represents the ratio of grain contact friction to inertial grain collision stress. At smaller values of this parameter, inter-granular stress terms play major role compared with the inertial term indicating that the effect of collision becomes major. At large values of the parameter, the inertial terms become important relatively to the inter-granular stress terms. This means that the turbulence of the mixture flows become dominant. Their works found that the velocity ratio (u/u_*) positively increases with the dimensionless parameter indicating that friction stress dominated flow mixture has a smaller velocity ratio while inertial stress dominated flow has a higher velocity ratio. This is theoretically understood because inertial stress dominated flow shows strong turbulence while friction stress dominated flow shows weak turbulence. Furthermore, we plotted the experimental data of Hashimoto and Hirano (1997), Jiangjia Ravine, and Kaimikahimorizawa (Figure 11), and found that stony flows distribute with the experimental data while velocity ratios of viscous flows decreases with the parameter. This finding was proved in works of Julien and Paris (2010) and further discussed by Yu (2012).

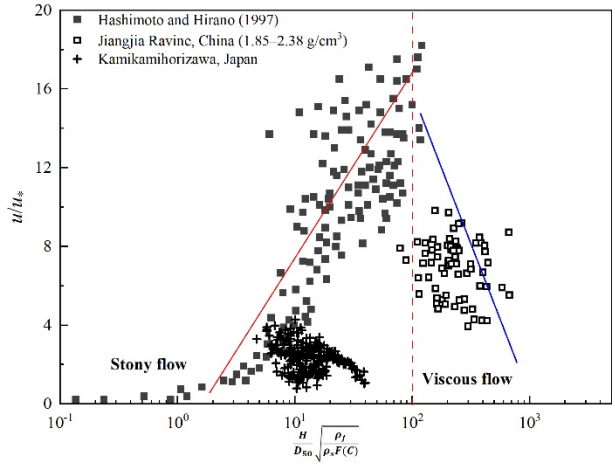

Figure 11. Plot exhibiting the the relationship between the relative average velocity of debris flow and relative flow depth.

The dimensionless analysis revealed that the Manning roughness coefficient strongly relates to the Friction number (Figures 9 and 10) and the viscous debris flows in Jiangjia Ravine and Wudu are mainly governed by friction stress

and secondly by viscous shear stress. For the stony flows in Kaimikahimorizawa, inertial stress plays a more important role than the friction stress. Considering the similar physical meanings of the parameter proposed by Hashimoto and Hirano (1997) and the Savage number, and the importance of the relative contact area of fine grains to flow column, we substitute H/D_{10} into Eq. (2) and the equation becomes:

$$\frac{H}{D_{10}}\sqrt{N_{\mathrm{Sav}}} = \frac{D_{50}}{D_{10}}\left(\frac{\mathrm{v}_s}{gtan\varphi(\rho_s-\rho_f)}\right)^{1/2} \#(10)$$

Correlating the eq. (10) with the velocity ratio can obtain:

$$\frac{u}{u_*} = 0.04\left(\frac{H}{D_{10}}\sqrt{N_{\mathrm{Sav}}}\right)^{0.65} \#(11)$$

$R^2 = 0.69$ (Figure 12)

Taking the shear velocity to right side and eq. (11) can be:

$$v = 0.008\left(\frac{D_{50}}{D_{10}}\right)^{0.96} \times \left(\frac{\rho_s}{\rho_s-\rho_f} \times \frac{1}{g\tan\varphi}\right)^{0.48} \times \ \mathrm{gHS}^{\ 0.74} \#(12)$$

The dot-black line in Figure 12 has higher R^2 than the dot-blue line, which is fitted by the supercritical flow data. We further verify the validity of the eq. (12) by the available data of debris flows of Jiangjia Ravine in 2006, the monitoring data of Houyenshan Ravine in 2012, and the debris flow monitoring data of Illgraben, Switzerland; Cancia, Italy; and Mount St. Helens, USA (Table 5). Among the six cases, debris flows at Mount St. Helens were triggered by volcanic eruption and should be termed as lahars. Such flows commonly have higher magnitude and runout distance than those at the other three sites. The results show that the calculated velocity in eq. (12) agrees well with the observed velocity (Figure 13), and this expression performs better than the methods in Table 1 (Figure 14).

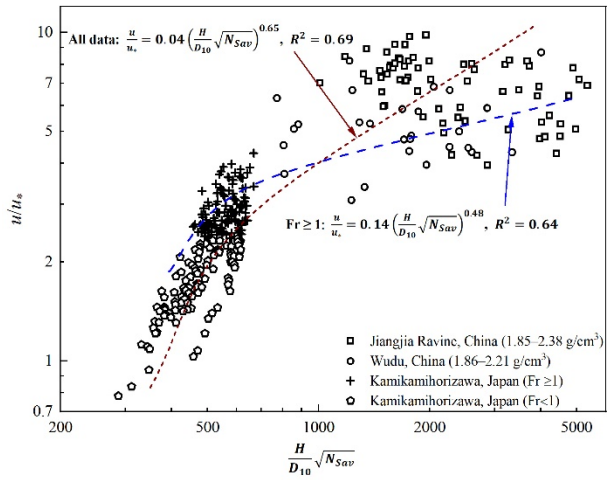

Figure 12. Plot exhibiting the the relationship between the improved relative average velocity of debris flow and relative flow depth.

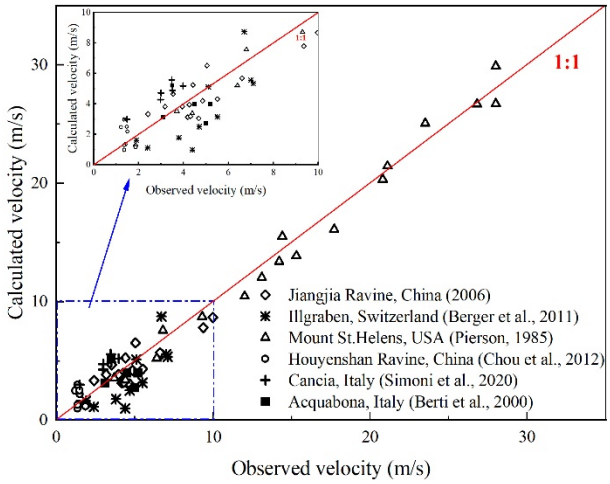

Figure 13. Plot illustrating the calculated velocity by the eq. (15) vs measured velocity

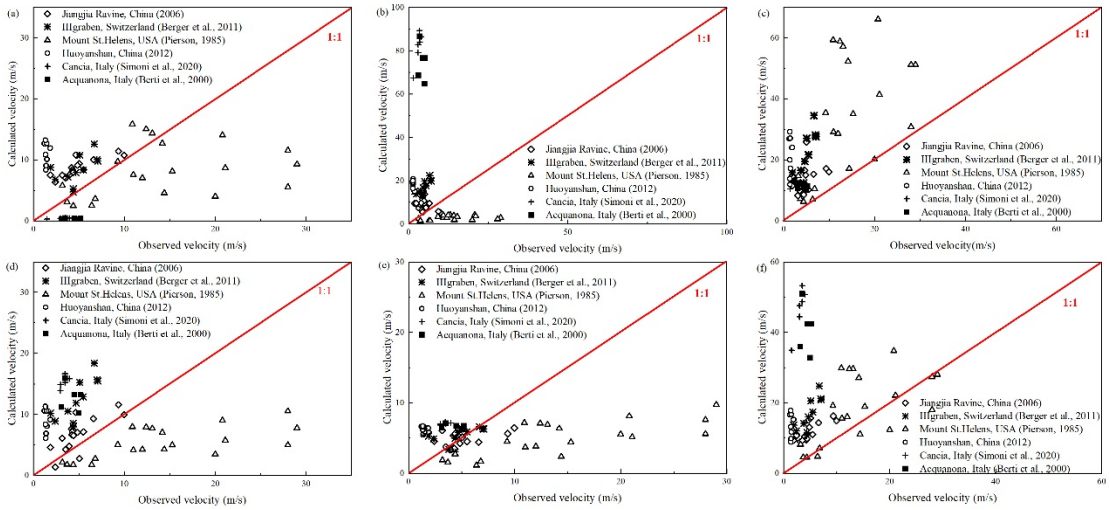

Figure 14. Plots depicting the calculated velocity by various methods in Table 1 vs measured velocity: (a) Kang (1985), (b) Fei (2003), (c) Julien and Paris (2010), (d) Yu (2012), (e) Hu et al. (2013), (f) Liu et al. (2020).

4 Discussions

Debris flow velocity is one of the most important parameters in mitigation measures design and some empirical methods and back-calculation approaches are proposed. Basically, the empirical methods are commonly derived from the Manning–Strickler method (Rickenmann, 1999). Along with the flow depth and channel gradient, the grain composition plays an important role (Cui et al., 2016; Liu et al., 2020). Table 1 lists some important methods globally and some scholars apply dimensionless analyses to examine the dynamic properties of debris flows. This work first collects the available debris flow data in some observation sites and analyzes the Manning coefficient, then correlates the Manning coefficient with dimensionless numbers to check the main component of resistance, and finally attempts to classify debris flows in the perspective of dominant stress and to develop a mean velocity equation of debris flows.

Among the three dimensionless numbers, the friction stress strongly relates to the Manning coefficient. If the friction stress acts by increasing contribution to the dynamics of debris flows, the Manning coefficient also increases thereafter. However, no such positive relationship exists for the other two dimensionless numbers. Furthermore, this work proposed debris flow classification on the basis of the dominant stress, and not other factors such as viscosity flow appearance or grain composition (Iverson & Denlinger, 2001; Takahashi, 1978). Such classification can be helpful to understand the main resistance component of debris flows (Table 3). Further, we proposed an index, D_{10}/H, to the friction number and found that it also closely relates to Manning coefficient. D_{10}/H is an index representing the relative contact area of fine grains (e.g., D_{10}/H) to

the flow column. The Friction number is the ratio between total friction stress and viscous shear stress. The friction stress interior debris flows is derived from the velocity differences between neighboring flow layer and can be burned by the coarse and fine grains. Therefore, D_{10}/H is meaningful in the analysis of debris flow resistance. Finally, we developed a new debris flow velocity equation based on the dimensionless index proposed by Hashimoto and Hirano (1997) and the Savage number. The new equation includes the D_{50}/D_{10}, shear velocity, and debris flow density. In comparison with the equation proposed by Yu and Tang (2016), the new equation involves the influence of debris flow density. The equation proposed by Julien and Paris (2010) does not involve D_{50}/D_{10} and debris flow density. As D_{50} and D_{10} represent the mean diameter and 10-percentile size, other characteristic diameter (D_x, x= 90, 86, 60, 16) representing the grain size of solid and fluid phases could be considered to develop a better method than eq. (12). Additionally, the debris flow data used for verifying eq. (15) involve friction stress-dominated debris flows in Jiangjia Ravine and Houyenshan, China; Illgraben, Switzerland; and Mount St. Helens, USA, and inertia-dominated flow in Acquabona Italy. The validity of eq. (15) may be verified in the future if the observed data is available for debris flows with various dominant stresses.

5 Conclusions

Debris flow velocity could be estimated using the Manning–Strickler method, while the relationship between Manning coefficient and the dominated stress of debris flow remains unclear. This study developed a unified mean velocity equation of debris flows on the basis of physical mechanics and provided new debris flow classifications. The following inferences were drawn:

The reciprocal Manning coefficients for viscous flows in Jiangjia are relatively higher while the reciprocal Manning coefficients for stony debris flows in Kamikamihorizawa and Ohya landslide, Japan are relatively small. The Manning coefficient can differ at the same observation site and given event.

The values of three dimensionless parameters reveal that the stony debris flows in Kamikamihorizawa are mainly governed by inertial stress and partially by friction stress, while the viscous debris flows in Jiangjia Ravine and Wudu, China, are mainly governed by frictional stress and partially by viscous shear stress. The reciprocal Manning coefficient of stony debris flows increases with the Savage and Bagnold numbers but not for viscous debris flows of China.

The reciprocal Manning coefficient decreases with the Friction number for both viscous and stony debris flows. We then proposed a debris flow classification by dominant stress according to the values of three dimensionless parameters. Finally, a new mean velocity equation of debris flows was proposed, in which the characterizing diameter equal to 50- and 10-percentile size, density, and shear velocity were used. This equation performed well and its validity can be updated in the future based on the availablity of the observed data of friction- and inertial stress-dominated flows.

Acknowledgments

All authors declare that no conflict of interest exists. This study was supported by the Second Tibetan Plateau Scientific Expedition and Research Program (grant No. 2019QZKK0902) and Fundamental Research Funds for the Central Universities (grant No. 2018BLCB). The authors sincerely thank Dr. Gordon G. D. Zhou for providing the data pertaining to the in-situ observation and measurement of debris flow at Jiangjia Ravine, Yunnan Province, China and other debris flow observations worldwide. We would like to thank Editage (www.editage.cn) for English language editing.

Author contributions:

Professor Chao Ma provided the data and methods used in this work and reviewed the current debris flow velocity equation. Master Lv Miao helped draw the figures under the guidance of Professor Chao Ma. Professor Cui Du provided the inspiration to investigate debris flow velocity through her previous works on the quadratic rheology model. Professor Lyu provided insightful comments on this work.

Data Availability Statement

The observed data of debris flow are from the Dongchuan debris flow observation station, Institute of mountai hazards and environment, Chinese academy of Science, and the book titled Research on debris flow in China on Science press China. Other debris flows data were obtained from documents online.

References

Arattano, M., & Franzi, L. (2004). Analysis of different water-sediment flow processes in a mountain torrent. *Natural Hazards and Earth System Sciences*, *4*(5/6), 783–791. https://doi.org/10.5194/nhess-4-783-2004

Armanini, A., Fraccarollo, L., & Rosatti, G. (2009). Two-dimensional simulation of debris flows in erodible channels. *Computers and Geosciences*, *35*(5), 993–1006. https://doi.org/10.1016/j.cageo.2007.11.008

Badoux, A., Graf, C., Rhyner, J., Kuntner, R., & McArdell, B. W. (2009). A debris-flow alarm system for the Alpine Illgraben catchment: Design and performance. *Natural Hazards*, *49*(3), 517–539. https://doi.org/10.1007/s11069-008-9303-x

Bagnold, R. A. (1954). Experiments on a gravity-free dispersion of large solid spheres in a Newtonian fluid under shear. *Proceedings of the Royal Society of London. Series A. Mathematical and Physical Sciences*, *225*(1160), 49–63. https://doi.org/10.1098/rspa.1954.0186

Bennett, G. L., Molnar, P., McArdell, B. W., & Burlando, P. (2014). A probabilistic sediment cascade model of sediment transfer

in the Illgraben. *Water Resources Research*, *50*(2), 1225–1244. https://doi.org/10.1002/2013WR013806

Berger, C., McArdell, B. W., & Schlunegger, F. (2011). Sediment transfer patterns at the Illgraben catchment, Switzerland: Implications for the time scales of debris flow activities. *Geomorphology*, *125*(3), 421–432. https://doi.org/10.1016/j.geomorph.2010.10.019

Berger, C., McArdell, B. W., & Schlunegger, F. (2011). Direct measurement of channel erosion by debris flows, Illgraben, Switzerland. *Journal of Geophysical Research: Earth Surface*, *116*(F1), n/a–n/a. https://doi.org/10.1029/2010JF001722

Berti, M., Genevois, R., LaHusen, R., Simoni, A., & Tecca, P. R. (2000). Debris flow monitoring in the Acquabona watershed on the dolomites (Italian Alps). *Physics and Chemistry of the Earth, Part B: Hydrology, Oceans and Atmosphere*, *25*(9), 707–715. https://doi.org/10.1016/S1464-1909(00)00090-3

Berti, M., Genevois, R., Simoni, A., & Tecca, P. R. (1999). Field observations of a debris flow event in the dolomites. *Geomorphology*, *29*(3–4), 265–274. https://doi.org/10.1016/S0169-555X(99)00018-5

Breien, H., De Blasio, F. V. D., Elverhøi, A., & Høeg, K. (2008). Erosion and morphology of a debris flow caused by a glacial lake outburst flood, western Norway. *Landslides*, *5*(3), 271–280. https://doi.org/10.1007/s10346-008-0118-3

Chou, H. T., Lee, C. F., Huang, C. H., & Chang, Y. L. (2012). The monitoring and flow dynamics of gravelly debris flows. *Journal of Chinese Soil and Water Conservation*, *44*(2), 144–157.

Chou, H.-T., Chang, Y.-L., & Zhang, S.-C. (2013). Acoustic signals and geophone response of rainfall-induced debris flows. *Journal of the Chinese Institute of Engineers*, *36*(3), 335–347. https://doi.org/10.1080/02533839.2012.730269

Coe, J. A., Kinner, D. A., & Godt, J. W. (2008). Initiation conditions for debris flows generated by runoff at Chalk Cliffs, central Colorado. *Geomorphology*, *96*(3–4), 270–297. https://doi.org/10.1016/j.geomorph.2007.03.017

Coussot, P., & Meunier, M. (1996). Recognition, classification and mechanical description of debris flows. *Earth-Science Reviews*, *40*(3–4), 209–227. https://doi.org/10.1016/0012-8252(95)00065-8

Cui, P., Guo, X. J., Yan, Y., Li, Y., & Ge, Y. G. (2018). Real-time observation of an active debris flow watershed in the Wenchuan Earthquake area. *Geomorphology*, *321*, 153–166. https://doi.org/10.1016/j.geomorph.2018.08.024

Cui, P., Tang, J. B., & Lin, P. (2016). Research progress of resistance character of debris-flow. Adv. *Engineering Sciences*, *48*, 1–11. https://doi.org/10.15961/j.jsuese.2016.03.001

Du, C. (2021). Deposition pattern of stony and muddy debris flow at the confluence area. *Journal of Mountain Science*, *18*(3), 622–634. https://doi.org/10.1007/s11629-020-6046-y

Du, R. H., Kang, Z. C., Chen, X. Q., & Zhu, P. Y. (1987). *Comprehensive investigation of debris flow in Xiaojiang, Yunnan and research on team governance planning*. Science and Technology Literature Press, pp. 94–141.

Fei, J., & Shu, A. (2004). *Movement mechanism of debris flow and disaster prevention*. Tsinghua University Press, pp. 114–144.

Fei, X. J. (2003). Velocity and solid transportation concentration of viscous debris flow. *Journal of Hydraulic Engineering*, *2*, 15–18. https://doi.org/10.3321/j.issn:0559-9350.2003.02.004

French, R. H. (1985). *Open-channel hydraulics*. New York: McGraw-Hill, pp. 163–195.

Hashimoto, H., & Hirano, M. (1997). Flow model of hyperconcentrated sand-water mixtures. In Proceedings of the 1997 1st international conference on Debris-Flow Hazards Mitigation: mechanics, prediction, and assessment, pp. 464–473. Reston, Virginia: ASCE.

Hu, K., Tian, M., & Li, Y. (2013). Influence of flow width on mean velocity of debris flows in wide open channel. *Journal of Hydraulic Engineering*, *139*(1), 65–69. https://doi.org/10.1061/(ASCE)HY.1943-7900.0000648

Hungr, O., Morgan, G. C., & Kellerhals, R. (1984). Quantitative analysis of debris torrent hazards for design of remedial measures. *Canadian Geotechnical Journal*, *21*(4), 663–677. https://doi.org/10.1139/t84-073

Imaizumi, F., Tsuchiya, S., & Ohsaka, O. (2005). Behaviour of debris flows located in a mountainous torrent on the Ohya landslide, Japan. *Canadian Geotechnical Journal*, *42*(3), 919–931. doi: 10.1139/t05-019

Iverson, R. M. (1997). The physics of debris flows. *Reviews of Geophysics*, *35*(3), 245–296. https://doi.org/10.1029/97RG00426

Iverson, R. M., & Denlinger, R. P. (2001). Flow of variably fluidized granular masses across three-dimensional terrain: 1. Coulomb mixture theory. *Journal of Geophysical Research: Solid Earth*, *106*(B1), 537–552. https://doi.org/10.1029/2000JB900329

Johnson, A. M. (1970). Mobilization of debris flows. *Zeitschrift für geomorphologie* (*Annals of Geomorphology*), Supplement, *9*, 168–186.

https://doi.org/10.1016/0148-9062(94)90792-7

Julien, P. Y. (2010). *Erosion and sedimentation*. Cambridge University Press, pp. 84–103.

Julien, P. Y., & Paris, A. (2010). Mean velocity of mudflows and debris flows. *Journal of Hydraulic Engineering*, *136*(9), 676–679. https://doi.org/10.1061/(ASCE)HY.1943-7900.0000224

Kang, Z. C. (1985). *A velocity analysis of viscous debris flow at Jiangjia Gully of Dongchuan in Yunnan*. Beijing: Memoirs of Lanzhou Institute of Glaciology and Cryopedology, Chinese Academy of Sciences, Science Press, pp. 108–118.

Kang, Z. C., Li, Z. F., & Ma, A. N. (2004). *Research on debris flow in china. Sci*. Press, pp. 212–240.

Li, Y. M., Ma, C., & Wang, Y. J. (2019). Landslides and debris flows caused by an extreme rainstorm on 21 July 2012 in mountains near Beijing, China. *Bulletin of Engineering Geology and the Environment*, *78*(2), 1265–1280. https://doi.org/10.1007/s10064-017-1187-0

Liu, D., Li, Y., You, Y., Liu, J., Wang, B., & Yu, B. (2020). Velocity of debris flow determined by grain composition. *Journal of Hydraulic Engineering*, *146*(8). https://doi.org/10.1061/(ASCE)HY.1943-7900.0001761, 6020010

Ma, C., Wang, Y. J., Hu, K. H., Du, C., & Yang, W. T. (2017). Rainfall intensity–duration threshold and erosion competence of debris flows in four areas affected by the 2008 Wenchuan earthquake. *Geomorphology*, *282*, 85–95. https://doi.org/10.1016/j.geomorph.2017.01.012

Marchi, L., Arattano, M., & Deganutti, A. M. (2002). Ten years of debris-flow monitoring in the Moscardo Torrent (Italian Alps). *Geomorphology*, *46*(1–2), 1–17. https://doi.org/10.1016/S0169-555X(01)00162-3

McCoy, S. W., Kean, J. W., Coe, J. A., Staley, D. M., Wasklewicz, T. A., & Tucker, G. E. (2010). Evolution of a natural debris flow: In situ measurements of flow dynamics, video imagery, and terrestrial laser scanning. *Geology*, *38*(8), 735–738. https://doi.org/10.1130/G30928.1

McCoy, S. W., Tucker, G. E., Kean, J. W., & Coe, J. A. (2013). Field measurement of basal forces generated by erosive debris flows. *Journal of Geophysical Research: Earth Surface*, *118*(2), 589–602. https://doi.org/10.1002/jgrf.20041

Mizuyama, T., & Uehara, S. (1984). Observed data of the depth and velocity of debris flow. *Journal of the Japan Society of Erosion Control Engineering*, *37*, 23–26.

Navratil, O., Liébault, F., Bellot, H., Travaglini, E., Theule, J., Chambon, G., & Laigle, D. (2013). High-frequency monitoring of debris-flow propagation along the Réal Torrent, Southern French Prealps. *Geomorphology*, *201*, 157–171. https://doi.org/10.1016/j.geomorph.2013.06.017

Okano, K., Suwa, H., & Kanno, T. (2012). Characterization of debris flows by rainstorm condition at a torrent on the Mount Yakedake volcano, Japan. *Geomorphology*, *136*(1), 88–94. https://doi.org/10.1016/j.geomorph.2011.04.006

Pierson, T. C. (1985). Initiation and flow behavior of the 1980 Pine Creek and Muddy river lahars, Mount St. Helens, Washington. *Geological Society of America Bulletin. Geological Society of America Bulletin*, *96*(8), 1056–1069. https://doi.org/10.1130/0016-7606(1985)96<1056:IAFBOT>2.0.CO;2

Rickenmann, D. (1999). Empirical relationships for debris flows. *Natural Hazards*, *19*(1), 47–77. https://doi.org/10.1023/A:1008064220727

Rickenmann, D., & Zimmermann, M. (1993). The 1987 debris flows in Switzerland: Documentation and analysis. *Geomorphology*, *8*(2–3), 175–189. https://doi.org/10.1016/0169-555X(93)90036-2

Savage, S. B., & Hutter, K. (1991). The dynamics of avalanches of granular materials from initiation to runout. Part I: Analysis. *Acta Mechanica*, *86*(1–4), 201–223. https://doi.org/10.1007/BF01175958

Shu, A. P., & Fei, X. J. (2003). Calculation for velocity and discharge of the viscous debris flow. *Journal of Sediment Research*, *3*, 7–11. https://doi.org/10.1007/BF02873153

Simoni, A., Bernard, M., Berti, M., Boreggio, M., Lanzoni, S., Stancanelli, L. M., & Gregoretti, C. (2020). Runoff-generated debris flows: Observation of initiation conditions and erosion–deposition dynamics along the channel at Cancia (eastern Italian Alps). *Earth Surface Processes and Landforms*, *45*(14), 3556–3571. https://doi.org/10.1002/esp.4981

Suwa, H., Okano, K., & Kanno, T. (2009). Behavior of debris flows monitored on test slopes of Kamikamihorizawa Creek, Mount Yakedake, Japan. *International Journal of Erosion Control Engineering*, *2*(2), 33–45. https://doi.org/10.13101/ijece.2.33

Takahashi, T. (1978). Mechanical characteristics of debris flow. *Journal of the Hydraulics Division*. American Society of Civil Engineers, 104(8), 1153–1169. https://doi.org/10.1061/JYCEAJ.0005046

Takahashi, T. (2007). *Debris flow: Mechanics, prediction and countermeasures*. CRC Press, pp. 33–70.

Takahashi, T., & Das, D. K. (2014). *Debris flow: Mechanics, prediction and countermeasures*. CRC Press, pp. 33–70.

Wang, Z., Hu, K. H., Ma, C., Li, Y., & Liu, S. (2021). Landscape change in response to multiperiod glacial debris flows in Peilong catchment, southeastern Tibet. *Journal of Mountain Science*, *18*(3), 567–582.

Wenner, M., Walter, F., McArdell, B., & Farinotti, D. (2019). *Deciphering debris-flow seismograms at Illgraben*. Switzerland: Colorado School of Mines. Arthur Lakes Library, pp. 1–7.

Yong, L., Xiaojun, Z., Pengcheng, S., Yingde, K., & Jingjing, L. (2013). A scaling distribution for grain composition of debris flow. *Geomorphology*, *192*, 30–42. https://doi.org/10.1016/j.geomorph.2013.03.015

Yu, B. (2012). Discussion of "mean velocity of mudflows and debris flows" by Pierre Y. Julien and Anna Paris. *Journal of Hydraulic Engineering*, *138*(2), 223–224. https://doi.org/10.1061/(ASCE)HY.1943-7900.0000480

Yu, B., & Tang, C. (2016). *Dynamics characteristics and activity law of debris flows*. Beijing: Science Press, pp. 35–60.

Zhou, G. G. D., & Ng, C. W. W. (2010). Dimensional analysis of natural debris flows. *Canadian Geotechnical Journal*, *47*(7), 719–729. https://doi.org/10.1139/T09-134

Zhu, X. H., Liu, B. X., & Liu, Y. (2020). New method for estimating roughness coefficient for debris flows. *Water*, *12*(9), 1–2545. https://doi.org/10.3390/w12092341

Table 1. *Empirical Formulae for Calculating Mean Velocity of Debris Flow*

No	Authors	Formulas	Data resources
1	Kang (1985)	$v = \frac{1}{n}H^{\frac{2}{3}}J^{\frac{1}{2}};\ \frac{1}{n} = 28.58H^{-0.34}$	Viscous flow in Jiangjia Ravine, China
2	Fei (2003)	$v = \frac{1}{n}H^{\frac{2}{3}}J^{\frac{1}{2}};\ \frac{1}{n} = 1.62\left[\frac{S_v(1-S_v)}{\sqrt{\mathrm{HJ}}D_{10}}\right]^{\frac{2}{3}}$	Viscous flow in Jiangjia Ravine and Hun
3	Julien and Paris (2010)	$\frac{u}{u_*} = 5.75\log\frac{H}{D_{50}}$	Collected debris flow data worldwide
4	Yu (2012)	$v = 3.2\sqrt{\mathrm{gHJ}}\log\frac{D_{50}}{D_{10}}$	All kinds flow in Jiangjia Ravine, Hunsh
5	Hu et al. (2013)	$v = 8.94H^{0.15}B^{0.35}J^{0.5}$	Viscous flow in Jiangjia Ravine, China
6	Liu et al. (2020)	$v = 4.04exp(2.59\mu)\left(\frac{H}{D_c}\right)^{\frac{1}{6}}\sqrt{\mathrm{gHJ}}$	All kinds flow in Jiangjia Ravine, China

Notes: v is mean velocity of debris flows (in m/s), H flow depth (in m), J channel gradient, n Manning coefficient, S_{v} volume fraction of debris flows, B flow depth (in m) ; u_* is shear velocity (in m/s) and is calculated by $(ghJ)^{1/2}$, g gravitation acceleration (9.8m/s^2); D_{50} and D_{10} are characteristic diameters equaling to the 50- and 10-percentile size (in mm); μ and Dc are two parameters

relating to debris flow density and characterizing parameter according to Yong et al. (2013).

Table 2. *Field Measured Flow Depth and Velocity, and Back-Calculated Manning Coefficient of Debris Flows in some Natural Sites.*

Watershed	h (m)	v (m/s)	$1/n$	References
Jiangjia Ravine, China	0.30 – 3.72	3.62 – 9.56	11.66 – 35.05	Kang et al. (2004)
Wudu, China	0.30 – 2.52	2.12 – 8.00	9.55 – 29.30	
Ohya landslide, Japan	0.29 – 0.76	2.34 – 3.50	5.59 – 9.29	Imaizumi et al. (2005)
Kamikamihorizawa, Japan	0.22 – 1.83	0.72 – 3.89	2.77– 15.26	Mizuyama & Uehara (1984); Suwa et
Moscardo, Italy	1.10 – 3.80	2.50 – 4.40	2.52 – 5.63	Marchi et al. (2002)
Acquabona, Italy	0.55 – 2.50	1.20 – 8.30	1.99 – 13.63	Berti et al. (1999)
Real Torrent, France	0.20 – 2.00	0.30 – 4.20	0.96 – 10.00	Navratil et al. (2013)
Illgraben, Switzerland	0.90 – 4.80	3.80 – 7.10	7.78 – 15.96	Berger et al. (2011); Wenner et al. (2
Chalk Cliff, USA	0.33 – 1.81	2.42 – 7.20	2.96 – 17.80	Coe et al. (2008)

Table 3. *The in situ Measured Bulk Density, Characteristic Diameter Equaling to 10– and 50– Percentile Size, and Viscosity of Debris Flow in Jiangjia Ravine and Wudu, China*

No	(g/cm^3)	D_{10}(mm)	D_{50}(mm)	(pa · s)	No	(g/cm^3)	D_{10}(mm)	D_{50}(mm)	(pa · s)	No	(
1	2.21	0.007	2.204	0.223	34	2.33	0.010	8.801	0.507	66	2.
2	2.19	0.007	0.553	0.204	35	1.89	0.004	5.656	0.058	67	2.
3	2.20	0.009	0.468	0.221	36	2.29	0.005	6.375	0.377	68	2.
4	2.25	0.008	2.630	0.290	37	2.02	0.004	1.506	0.093	69	0.
5	2.21	0.009	1.706	0.228	38	1.92	0.002	0.268	0.064	70	1.
6	2.20	0.011	7.909	0.218	39	1.88	0.003	1.199	0.056	71	2.
7	2.21	0.011	8.891	0.232	40	2.15	0.004	1.844	0.166	72	2.
8	2.22	0.010	7.706	0.243	41	2.09	0.003	0.947	0.125	73	0.
9	2.20	0.009	6.406	0.218	42	2.07	0.004	1.506	0.115	74	0.
10	2.21	0.010	7.950	0.228	43	2.10	0.003	0.576	0.131	75	0.
11	2.19	0.009	7.054	0.204	44	2.21	0.003	1.602	0.226	76	1.
12	2.21	0.007	0.312	0.223	45	2.15	0.003	1.438	0.164	77	0.
13	2.21	0.009	7.527	0.230	46	2.08	0.003	1.697	0.118	78	1.
14	2.25	0.008	7.846	0.283	47	2.02	0.003	0.467	0.094	79	0.
15	2.25	0.009	7.991	0.294	48	1.87	0.002	0.047	0.054	80	0.
16	2.25	0.009	7.666	0.290	49	2.14	0.003	1.005	0.156	81	0.
17	2.24	0.010	8.799	0.271	50	2.20	0.003	1.627	0.215	82	1.
18	2.28	0.010	8.309	0.343	51	2.24	0.003	1.996	0.279	83	0.
19	2.12	0.006	6.236	0.145	52	2.01	0.002	0.290	0.089	84	0.
20	2.29	0.010	8.573	0.365	53	1.89	0.002	0.540	0.058	85	0.
21	2.20	0.007	6.050	0.221	54	2.23	0.003	0.676	0.251	86	2.
22	2.21	0.008	7.315	0.226	55	2.17	0.004	2.438	0.184	87	1.

No	(g/cm^3)	D_{10}(mm)	D_{50}(mm)	(pa · s)	No	(g/cm^3)	D_{10}(mm)	D_{50}(mm)	(pa · s)	No	(
23	2.27	0.012	9.414	0.323	56	2.17	0.003	1.118	0.182	88	0.
24	2.21	0.008	7.277	0.232	57	2.05	0.003	1.248	0.105	89	1.
25	2.22	0.008	6.908	0.242	58	2.12	0.004	2.286	0.146	90	0.
26	2.07	0.006	4.584	0.114	59	2.25	0.004	2.127	0.283	91	0.
27	2.09	0.003	4.239	0.125	60	2.07	0.003	0.768	0.113	92	0.
28	2.15	0.002	2.219	0.166	61	2.13	0.003	1.753	0.148	93	0.
29	2.15	0.003	5.295	0.166	62	1.95	0.004	1.636	0.072	94	0.
30	2.24	0.009	8.844	0.273	63	2.11	0.004	2.101	0.138	95	1.
31	2.21	0.005	6.961	0.228	64	2.19	0.003	1.772	0.204	96	0.
32	2.24	0.013	10.416	0.273	65	2.17	0.004	2.101	0.182	97	1.
33	2.14	0.005	7.490	0.154							

Note: Data no. 1–57 are from debris flow observation station at Jiangjia Ravine, and data no. 58–97 are observed data in Wudu, China.

Table 4. *Three Dimensionless Numbers and the Dominant Stress of Debris Flows in Natural Observation Sites*

Dominant stress	Watershed/debris flow site	N_{Bag} (10^3)	N_{Sav} (10^{-4})	N_{Fric} (10^4)
Friction stress	Oddstad debris flow	4.00×10^3	2.00	2.00
	South Toutle River	2.00×10^4	0.06	3.00
	Osceola Mudflow	4.00×10^4	1.0010^{-3}	40.00
	Illgraben, Switzerland	0.20–4.00	10.00–40.00	2.30–47.40
	Jiangjia Ravine, China	-	$0.26–0.29\times10^3$	0.02–3.02
	Houyenshan Ravine, China	0.60	50.00	12.70
	Jiangjia Ravine, China	5.0010^{-5}–0.02	0.02–8.89	0.13–5.40
	WuDu, China	2.00×10^{-3}–0.11	0.33–27.00	0.09–6.08
Inertial stress	Acquabona, Italy	2.50–18.00	0.20×10^3–9.30×10^3	1.90–12.80
	Moscardo, Italy	5.70–46.00	0.10×10^3–1.9610^4	2.30–47.40
	Chalk Cliff, Central Colorado, USA	4.40	1.90×10^3	2.40
	Kamikamihorizawa, Japan	6.60–64.87	0.22×10^3–1.6210^4	0.34–78.10

Table 5. *Collected Debris Flow Data for Mean Velocity Equation Verification*

Watershed	(g/cm^3)	h (m)	v (m/s)	D_{10} (mm)	D_{50} (mm)	References	Wate
Jiangjia Ravine, China	2.21	1.50	9.97	0.014	9.550	Observed data	Moun
	2.23	1.80	9.36	0.421	12.720		
	2.17	1.50	4.68	0.322	8.172		
	2.02	1.20	6.61	0.155	5.458		
	2.23	0.80	4.19	0.228	7.110		

Watershed	(g/cm^3)	h (m)	v (m/s)	D_{10} (mm)	D_{50} (mm)	References	Wate
	2.26	0.70	4.31	0.224	7.230		
	2.10	0.50	3.18	0.123	5.294		
	1.99	0.50	1.87	0.059	1.855		
	1.71	1.00	5.05	0.011	0.439		
	2.22	0.60	4.26	0.176	6.614		
	2.08	0.60	4.42	0.180	8.263		
	2.01	0.70	5.51	0.150	6.204		
	1.91	0.90	4.85	0.053	1.988		
	1.79	0.40	3.54	0.037	2.053		
	1.79	0.50	3.95	0.020	0.960		
	1.50	0.30	2.42	0.005	0.280		
Illgraben, Switzerland	2.10	4.80	6.70	0.008	5.282	Berger et al. (2011)	
	2.10	3.30	5.10	0.008	5.282		
	2.10	3.40	7.10	0.008	5.282		Houy
	2.10	3.50	7.00	0.008	5.282		
	2.10	2.00	4.69	0.008	5.282		
	2.10	1.13	2.40	0.008	5.282		
	2.10	2.35	5.50	0.008	5.282		
	2.10	1.47	1.90	0.008	5.282		
	2.10	1.04	4.40	0.008	5.282		
	2.10	1.57	3.80	0.008	5.282		
Cancia, Italy	1.75	1.70	1.48	0.910	26.550	Simoni et al. (2020)	Acqua
	1.75	3.95	3.48	0.910	26.550		
	1.75	3.15	2.99	0.910	26.550		
	1.75	3.58	3.98	0.910	26.550		
	1.75	2.75	2.98	0.910	26.550		